Supplementary Material

Table of contents:

Supplementary Tables

Supplementary Table 1. Bone Marrow cellularity estimates retrieved from literature for human and mice using different techniques

BM Cellularity (cells/Kg BW)	Reference	Species
1.96E+10	Colvin et al 2004 (1)	Mice - BALB/c (mean BW 23g)
1.94E+10	Colvin et al 2004 (1)	Mice - C57/BLK (mean BW 24g)
1.25E+10	Colvin et al 2004 (1)	Mice - DBA/2 (mean BW 22.65g)
1.20E+10	Boggs et al. 1984 (2)	Mice - B6D2fl (mean BW 23.5g)
8.10E+09	Pegg 1962 (3)	Human
4.60E+10	Osgood 1954 (4)	Human
1.36E+10	Patt 1957 (5)	Human
1.80E+10	Donohue et al. 1958 (6)	Human
1.11E+10	Harrison et al. 1962 (7)	Human
1.04E+10	Harrison et al. 1962 (7)	Human
2.01E+10	Skarberg et al 1974 (8)	Human
7.70E+09	Suit 1957 (9)	Human

Supplementary Figures

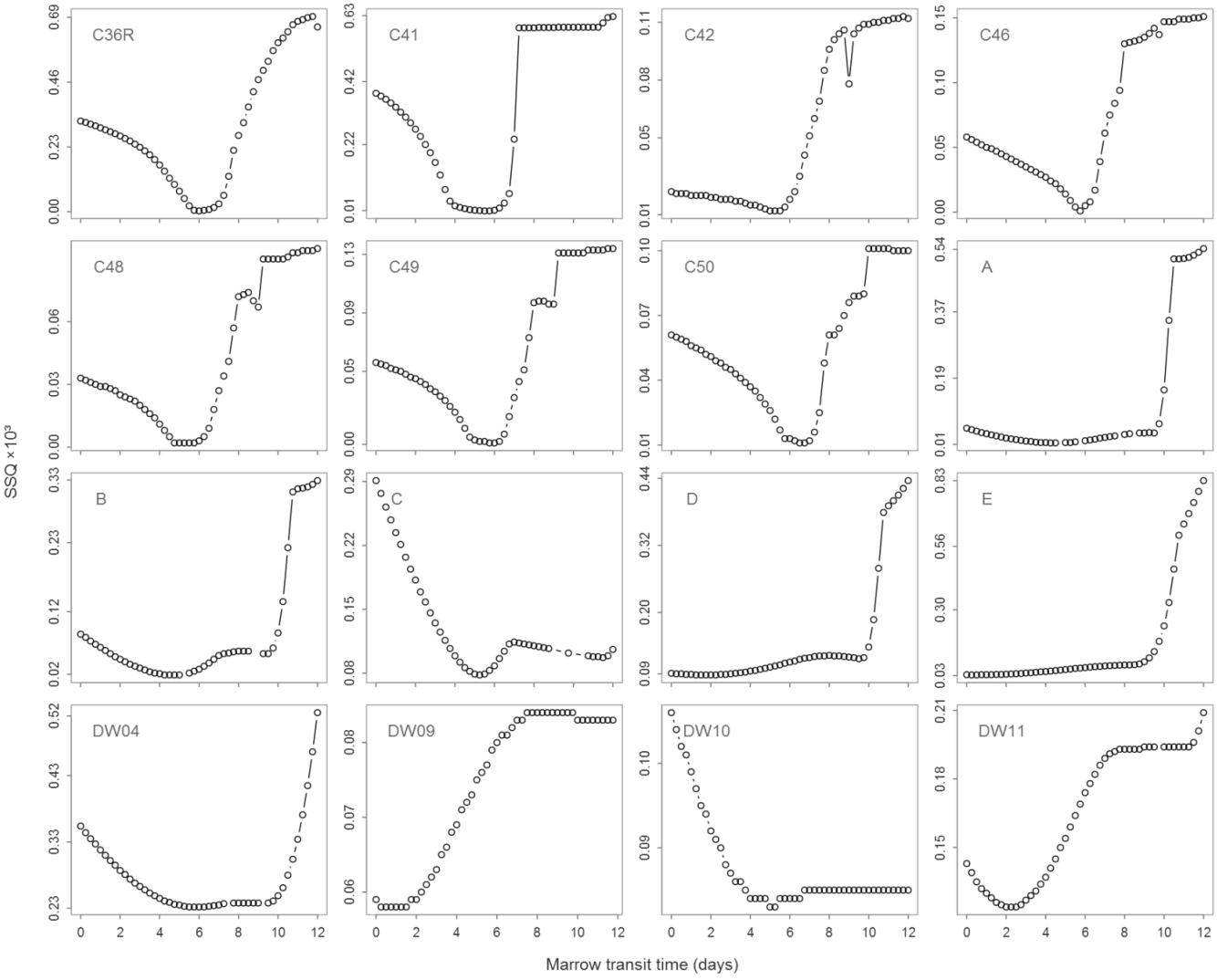

Supplementary Figure 1: Sum of squares as a function of marrow transit time.

Neutrophil loss rate from blood (and b_w in the case of labeling with water) were free parameters whereas marrow transit time was fixed to given values (abscise axis). The minima indicate the numerically most-plausible scenarios. The first 7 panels (Subjects C36R-C50) are from subjects labeled with deuterated glucose; the remaining 9 panels (Subjects A-E and DW04-DW11) are from subjects labeled with heavy water.

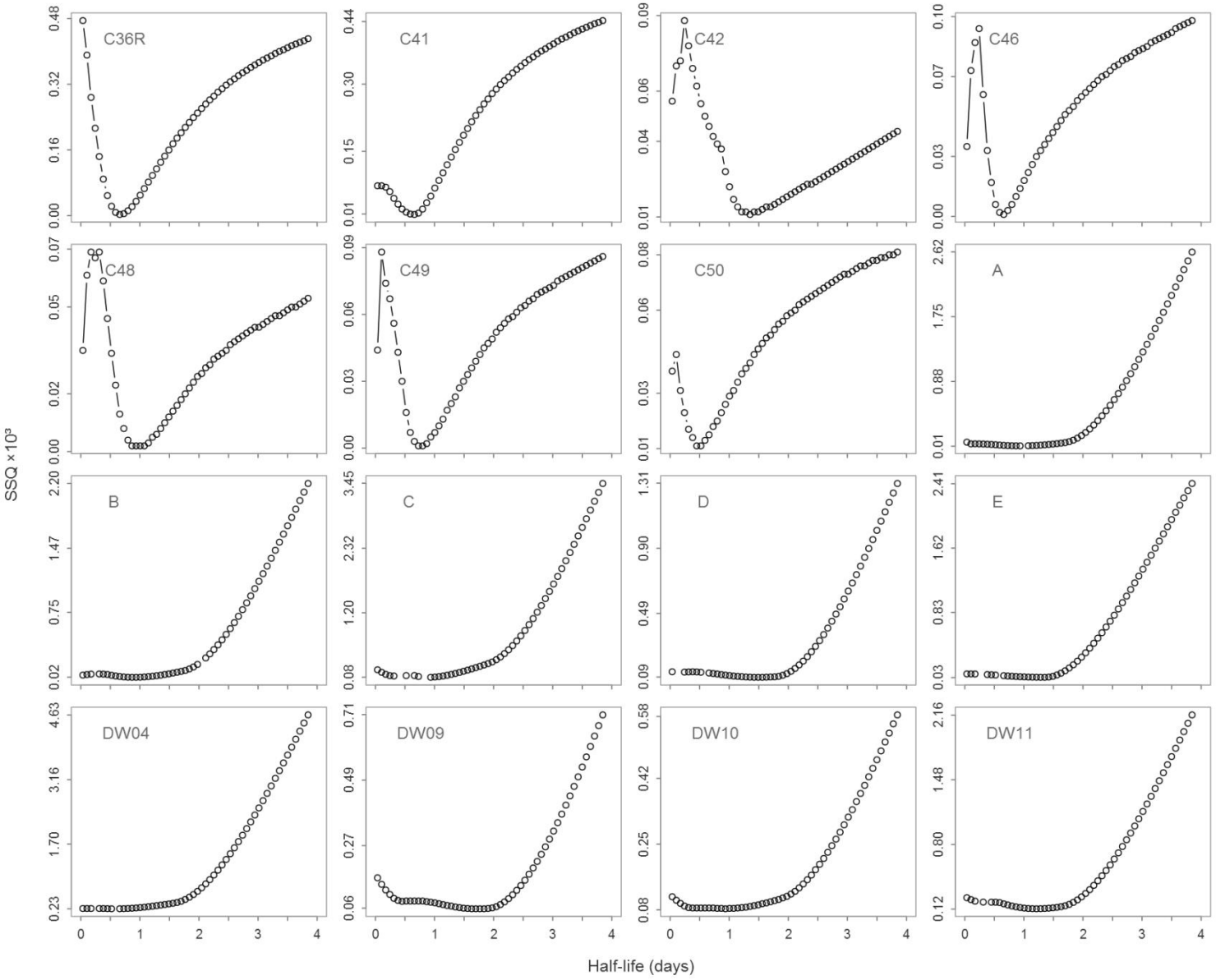

Supplementary Figure 2: Sum of squares as a function of half-life.

Marrow transit time (and b_w in the case of labeling with water) were free parameter whereas loss rate from blood was fixed to the given values (abscise axis, expressed as a half-life). The minima indicate the numerically most-plausible scenarios. The first 7 panels (Subjects C36R-C50) are from subjects labeled with deuterated glucose; the remaining 9 panels (Subjects A-E and DW04-DW11) are from subjects labeled with heavy water.

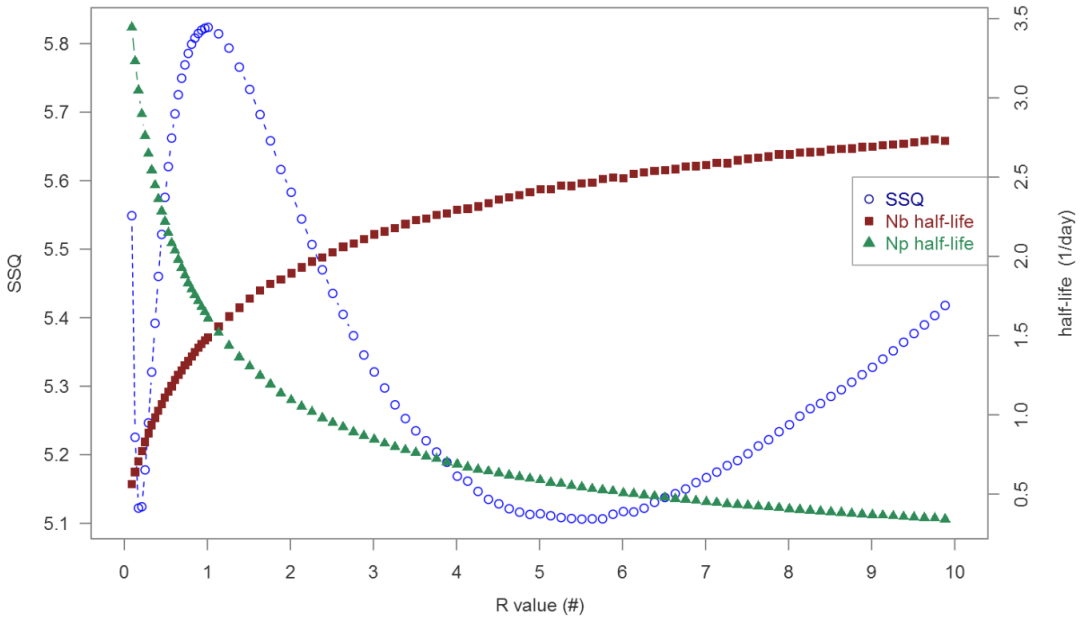

Supplementary Figure 3: Sum of squares and half-life estimates as a function of R.

The model was simultaneously fitted to data from the 9w heavy water labeling study, 10h and 3h deuterium-labeled glucose labeling study. Marrow transit-time and neutrophil loss rate from blood were free parameters, whereas R was fixed to given values (see abscises axis). The resulting sum of squares and half-life estimates (for both bone marrow neutrophil precursors and blood neutrophils) are plotted. The minima in the SSQ indicate the numerically most-plausible scenarios.

Supplementary Figure 4. Effect of secondary purification on neutrophil DNA enrichment curves

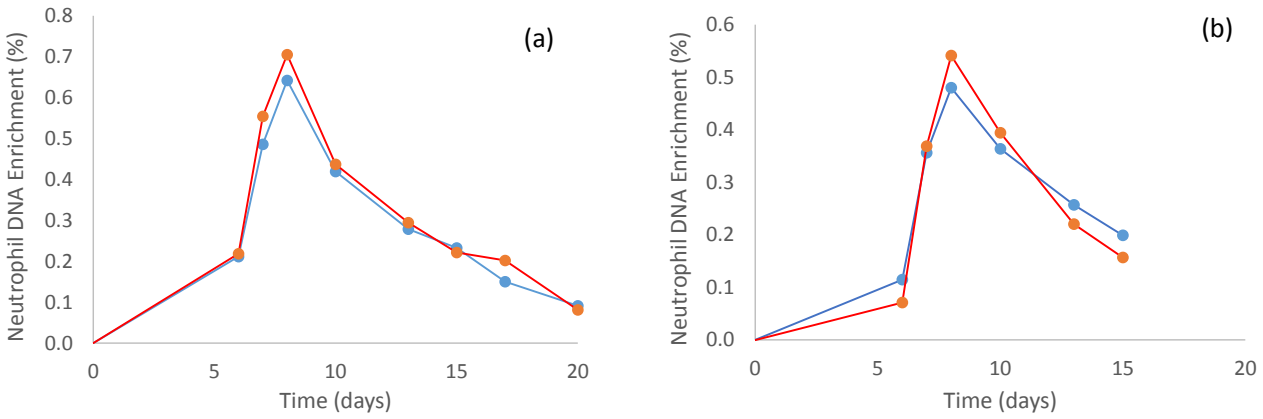

In two subjects, C59 and C60, aliquots were further purified by CD16 antibody-coated magnetic bead adhesion (Miltenyi Biotec, UK) and analyzed in parallel with cells purified by gradient-separation alone. Neutrophil DNA Enrichment curves for C59 (a) and C60 (b). Cells were separated by gradient-centrifugation in Polymorphprep, either alone (blue lines) or with a subsequent CD16 microbead separation (red lines).

Supplementary Text 1: Deuterium-labeled glucose plasma exposure

For the 3h, 4h and 10h labelling protocols U_t was approximated by the following function:

$$U_t = MAPE_{(0-\tau)} \qquad if\ (t \leq \tau)$$

$$U_t = APE_\tau \cdot e^{-k_d \cdot (t-\tau)} \qquad if\ (t > \tau)$$

where τ is the time of the last dose, $MAPE_{(0-\tau)}$ is the mean plasma enrichment between time 0 and τ (calculated as the area under the plasma enrichment curve divided by τ), APE_τ is the plasma enrichment at time τ and k_d is the elimination constant of glucose for each individual. Parameter values are given in Supplementary Table 2.

For the bolus-dose labelling protocol, U_t was approximated by interpolating between each data point (see Supplementary Figure 5).

Supplementary Table 2. Exposure parameters for individuals from the 3h, 4h and 10h glucose labelling protocols

Identifier	MAPE (%)	APE_tau (%)	k_d (h-1)	Tau, τ (h)
C36R	27.3	22.4	0.856	10
C41	41.6	39.9	0.589	10
C42	39.8	49.5	0.580	4
C46	25.9	33.9	0.468	3
C48	31.8	40.5	0.596	3
C49	37.7	27.9	0.610	3
C50	12.0	20.9	0.371	3

Supplementary Figure 5. Deuterium-labeled glucose exposure curves for C59 and C60

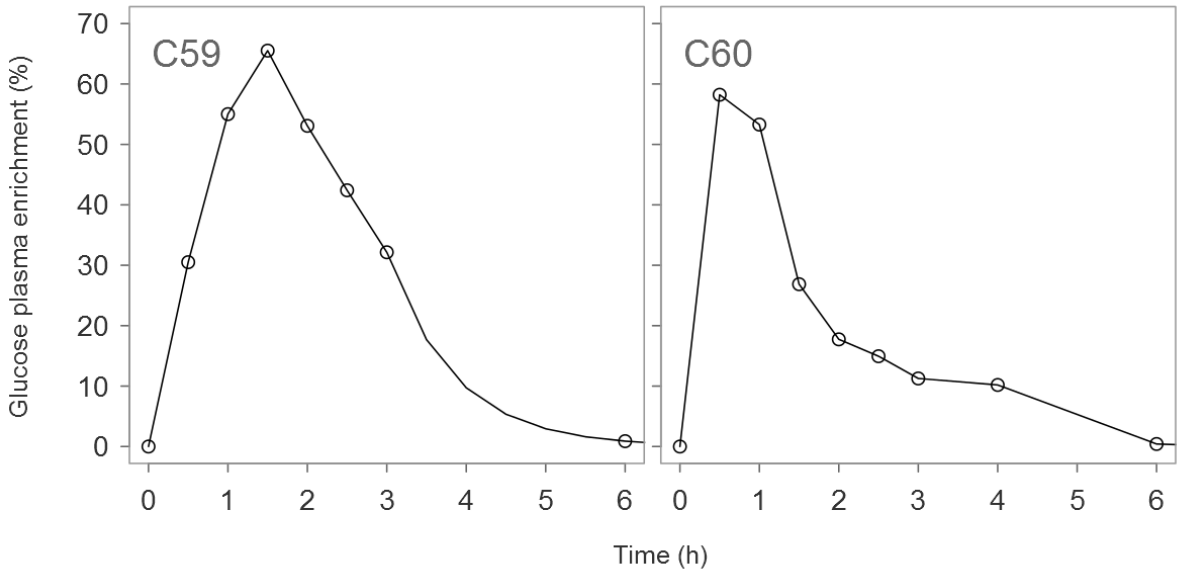

Graphs show plasma glucose deuterium enrichment for subjects C59 and C60. For C59, points between 3h and 6h were estimated using linear interpolation on a log linear scale. After 7h label exposure was considered to be negligible.

Supplementary Text 2: Comparison between model used by Pillay *et al* and the two-compartment model developed here

Pillay et al. model

The model used by Pillay et al. (10) describes granulocyte turnover in terms of proliferation and death in a single homogenous compartment at steady state. The equation is as follows:

$$\frac{dL_b}{dt} = z \cdot b \cdot U_{(t-\Delta)} - z \cdot L_b \qquad (1)$$

where b is the heavy water normalizing factor, z is the proliferation/death rate (equal at steady-state) and Ut is the label availability function at time t, in this equation lagged by a parameter Δ.

Consider a square pulse of label such that U_t is a step function (U_t=A if time is smaller or equal than the labelling time (τ), and 0 once label administration has finished). In such a scenario equation 1a can be discretized to the following:

$$\frac{dL_b}{dt} = 0 \qquad if\ t \leq \Delta \qquad (2a)$$

$$\frac{dL_b}{dt} = z \cdot b \cdot A - z \cdot L_b \qquad if\ \Delta < t < \tau + \Delta \qquad (2b)$$

$$\frac{dL_b}{dt} = -z \cdot L_b \qquad if\ t \geq \tau + \Delta \qquad (2c)$$

Two-compartment model

Our model, in contrast to that of Pillay et al. model, describes granulocyte turnover using two compartments (see main text Figure 1). Model equations are the following:

$$\frac{dL_p}{dt} = z \cdot R \cdot b \cdot U_{(t)} - z \cdot R \cdot L_p \qquad (3a)$$

$$\frac{dL_b}{dt} = z \cdot L_p(t - \Delta) - z \cdot L_b \qquad (3b)$$

Assuming a step function for U_t, as before, and solving 3a analytically we obtain equations 4a and 4b.

$$L_p(t) = b \cdot A \cdot (1 - e^{-z \cdot R \cdot t}) \qquad if\ t \leq \tau \qquad (4a)$$

$$L_p(t) = b \cdot A \cdot (1 - e^{-z \cdot R \cdot \tau}) e^{-R \cdot z(t-\tau)} \qquad if\ t > \tau \qquad (4b)$$

Substituting these into 3b we obtain

$$\frac{dL_b}{dt} = 0 \qquad if\ t \leq \Delta \qquad (5a)$$

$$\frac{dL_b}{dt} = z \cdot b \cdot A \cdot \left(1 - e^{-z \cdot R \cdot (t-\Delta)}\right) - z \cdot L_b \qquad if\ \Delta < t < \tau + \Delta \qquad (5b)$$

$$\frac{dL_b}{dt} = z \cdot b \cdot A \cdot (1 - e^{-z \cdot R \cdot \tau}) e^{-R \cdot z \cdot (t-\tau-\Delta)} - z \cdot L_b \qquad if\ t > \tau + \Delta \qquad (5c)$$

Comparing (5a)-(5c) with (2a)-(2c), we see that as R tends to infinity our model is mathematically identical to the model of Pillay *et al.* It can thus be seen that Pillay *et al* implicitly assume that R is large, an assumption which appears to be at odds with current knowledge of the system. Furthermore, it can be seen (Supplementary Figure 3) that as R is increased the estimate of the circulating half-life increases, explaining why Pillay *et al* obtained such large estimates for the half life.

Supplementary Material References

1. Colvin G, Lambert J, Abedi M, Hsieh C, Carlson J, Stewart F, et al. Murine marrow cellularity and the concept of stem cell competition: geographic and quantitative determinants in stem cell biology. Leukemia. 2004;18(3):575-83.
2. Boggs D. The total marrow mass of the mouse: a simplified method of measurement. American journal of hematology. 1984;16(3):277-86.
3. Pegg D. A quantitative study of bone marrow grafting: Implications for human bone marrow infusion. British journal of cancer. 1962;16(3):400.
4. Osgood EE. Number and distribution of human hemic cells. Blood. 1954;9(12):1141-54.
5. Patt HM. A consideration of myeloid-erythroid balance in man. Blood. 1957;12(9):777-87.
6. Donohue DM, Gabrio BW, Finch CA. Quantitative measurement of hematopoietic cells of the marrow. Journal of Clinical Investigation. 1958;37(11):1564.
7. Harrison W. The total cellularity of the bone marrow in man. Journal of clinical pathology. 1962;15(3):254-9.
8. Skårberg KO. Cellularity and cell proliferation rates in human bone marrow. Acta medica Scandinavica. 1974;195(1-6):291-9.
9. Suit H. A technique for estimating the bone marrow cellularity in vivo using 59Fe. Journal of clinical pathology. 1957;10(3):267.
10. Pillay J, den Braber I, Vrisekoop N, Kwast LM, de Boer RJ, Borghans JA, et al. In vivo labeling with 2H2O reveals a human neutrophil lifespan of 5.4 days. Blood. 2010;116(4):625-7.
11. Jilma B, Hergovich N, Stohlawetz P, Eichler HG, Bauer P, Wagner O. Circadian variation of granulocyte colony stimulating factor levels in man. British journal of haematology. 1999;106(2):368-70.
12. Akbulut H, Icli F, Büyükcelik A, Akbulut KG, Demirci S. The role of granulocyte-macrophage-colony stimulating factor, cortisol, and melatonin in the regulation of the circadian rhythms of peripheral blood cells in healthy volunteers and patients with breast cancer. Journal of pineal research. 1999;26(1):1-8.
13. Smaaland R, Laerum O, Lote K, Sletvold O, Sothern R, Bjerknes R. DNA synthesis in human bone marrow is circadian stage dependent. Blood. 1991;77(12):2603-11.
14. Smaaland R, Laerum O, Sothern R, Sletvold O, Bjerknes R, Lote K. Colony-forming unit-granulocyte-macrophage and DNA synthesis of human bone marrow are circadian stage-dependent and show covariation. Blood. 1992;79(9):2281-7.
15. Granda TG, Liu X-H, Smaaland R, Cermakian N, Filipski E, Sassone-Corsi P, et al. Circadian regulation of cell cycle and apoptosis proteins in mouse bone marrow and tumor. The FASEB Journal. 2005;19(2):304-6.
16. Casanova-Acebes M, Pitaval C, Weiss LA, Nombela-Arrieta C, Chèvre R, Noelia A, et al. Rhythmic modulation of the hematopoietic niche through neutrophil clearance. Cell. 2013;153(5):1025-35.
17. Furze RC, Rankin SM. The role of the bone marrow in neutrophil clearance under homeostatic conditions in the mouse. The FASEB Journal. 2008;22(9):3111-9.
18. Slayter KL, Ludwig EA, Lew KH, Middleton E, Ferry JJ, Jusko WJ. Oral contraceptive effects on methylprednisolone pharmacokinetics and pharmacodynamics. Clinical Pharmacology & Therapeutics. 1996;59(3):312-21.